Ab Initio Coupled Hartree−Fock Investigation of the Static First Hyperpolarizability of Model *all-trans*-Polymethineimine Oligomers of Increasing Size

Benoît Champagne,*,† Denis Jacquemin,‡ and Jean-Marie André

Laboratoire de Chimie Théorique Appliquée, Facultés Universitaires Notre-Dame de la Paix, 61 rue de Bruxelles, B-5000 Namur, Belgium

Bernard Kirtman

Chemistry Department, University of California, Santa Barbara, California 93106

Received: September 9, 1996[⊗]

The static first hyperpolarizability tensor of model *all-trans*-polymethineimine oligomers has been computed *ab initio* as a function of chain length using the coupled Hartree−Fock method with the 6-31G basis. Careful extrapolations were carried out to obtain reliable infinite polymer values per unit cell. For the most realistic structure the longitudinal component is about 4 times larger than any other and is of the same order of magnitude as in push−pull polyenes. A plot of this component vs chain length exhibits a characteristic "dromedary back" shape. The role of bond alternation and heteroatomicity in determining this shape through their effect on the electronic delocalization and two different types of asymmetry (backbone, chain end) is examined qualitatively as well as quantitatively. It is shown that the correct chain length dependence is not reproduced by the uncoupled Hartree−Fock approximation.

1. Introduction

Quantum chemistry can play a crucial role in the design of new materials for nonlinear optics (NLO) applications.[1−3] The computation of NLO properties, as well as their interpretation in terms of chemical structure−property relationships, provides an efficient means for directing synthetic efforts. Many theoretical papers have addressed the first hyperpolarizability, β, of organic molecules. This molecular property, responsible for the dc-Pockels effect and the second harmonic generation, has been evaluated for a wide range of molecules of potential interest for NLO applications. It has been shown that a large first hyperpolarizability can result from combining donor and acceptor groups separated by a conjugated linker. Many donors and acceptors have been tested as well as different types of linkers.[4−13] For most of these systems, the two-state approximation[2,14−15] appears to correctly reproduce *trends* in the first hyperpolarizability upon substitution and/or upon modification of the linker. This is because the first-order nonlinear response is often due primarily to a single charge-transfer excited state. The interplay between the strength of the donor−acceptor pair, the length of the linker, and the polarity of the solvent open many directions for tuning the linear and nonlinear response.[11−13,16−20] A simple model based on the simulation of solvent and donor−acceptor effects by a uniform external electric field has been used to give a unified description of the linear and nonlinear response in this class of molecules.[16−19]

On the other hand, there have been only a few studies of the first hyperpolarizabilities in oligomeric or polymeric chains. This is because most of the systems considered[21−22] are centrosymmetric which implies a zero β value. To our knowledge β has been obtained only for polymethineimine (PMI)[23−25] and polyaniline[26] chains and, in those cases, only at an empirical or

semiempirical level. Albert *et al.*[23] treated small *all-trans*-PMI chains (2−5 unit cells) within the Pariser−Parr−Pople (PPP) scheme. Their longitudinal β values are larger than the NLO responses of push−pull polyenes with a push-pull strength of 1.0 eV. The size-dependence relation $\beta = cN^{3.04}$ obtained from these oligomeric results (N is the number of unit cells and c is a constant) suggested that the asymptotic linear evolution with respect to chain length would be slowly attained. Using the perturbative expansion of the density matrix (PEDM) method and a PPP treatment, Sales *et al.*[26] have shown that the longitudinal first hyperpolarizability of polyaniline oligomers strongly increases upon going from the totally reduced or leucoemeraldine form to the fully oxidized or pernigraniline form. Unfortunately, their study did not involve sufficiently large oligomers to address the chain length dependence. Although the above results are only of a suggestive nature, it is still surprising that the substantial first hyperpolarizability computed by Albert *et al.*[23] and Sales *et al.*[26] has not yet given rise to experimental investigations of these noncentrosymmetric conjugated organic polymers.

Recently, we began a comprehensive study of the first hyperpolarizability of the PMI. This polymer, which was synthesized a quarter of a century ago,[27−28] may also be considered as a model for other analogous heteroatomic systems. Initially, Hückel calculations of the static longitudinal component per unit cell, $\Delta\beta_{zzz}$, were carried out for finite and infinite chains.[24] The evolution with chain length of $\Delta\beta_{zzz}$ shows a maximum for short chains and then decreases until the asymptotic value is reached. By varying the Hückel parameters it was shown that increasing the bond alternation reduces $\Delta\beta_{zzz}$ at the maximum and leads to a more rapid convergence to the asymptotic limit. The rate of convergence increases with heteroatomicity as well. An increase in the latter also results in a more rapid attainment of the maximum in $\Delta\beta_{zzz}$ as a function of chain length. We have explained the behavior of $\Delta\beta_{zzz}$ qualitatively in terms of the antagonistic effects of either the heteroatomicity or the bond alternation upon the delocalization of the electron distribution and its asymmetry. There is always

all-trans-Polymethineimine Oligomers

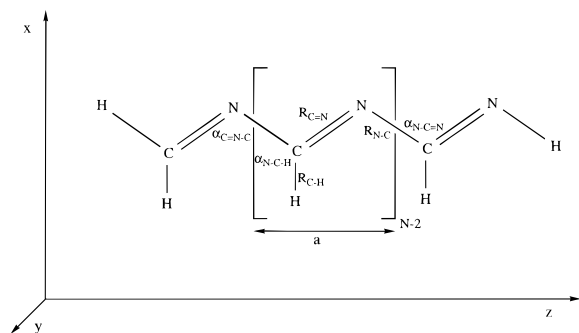*J. Phys. Chem. A, Vol. 101, No. 17, 1997* **3159**

Figure 1. Structure of the PMI chains, which are oriented so that the line connecting the midpoint of the C=N bonds is parallel to the *z* axis.

a limiting factor, either the electron delocalization or the asymmetry, which depends not only upon the relative hetero-atomicity and bond alternation values but also upon the chain length.

Since the Coulombic interactions are not explicitly taken into account in the Hückel approach, all levels of approximation are reduced to the uncoupled Hartree–Fock (UCHF) scheme. In the second paper of the series[25] we used PPP Hamiltonians to incorporate the field-induced electron reorganization effects by means of the coupled Hartree–Fock (CHF) method. Two different PPP parametrizations were employed. The more realistic one corresponds to greater delocalization. It yields the same "dromedary back" shape for the plot of $\Delta\beta_{zzz}$ vs chain length as the Hückel calculation but gives a large negative (!) longitudinal first hyperpolarizability in the asymptotic limit (the other in-plane components are much smaller in magnitude). The corresponding PPP/UCHF calculation reproduces the shape of the curve but leads to a limiting value of $\Delta\beta_{zzz}$ that is close to zero. A satisfactory explanation of the behavior in the vicinity of the maximum is provided by a new UCHF sum-over-states approximation scheme, although the latter fails just like the conventional *N*-level treatment at longer chain lengths. In this new scheme, the two largest terms are of opposite sign; the negative one is smaller in amplitude for the shortest chains but increases more rapidly with chain length thereby producing a maximum. The failure of either approach for long chains may be attributed to the fact that many excitations contribute substantially to the first hyperpolarizability since each unit cell contains one donor and one acceptor group and constitutes, at the same time, a part of the conjugated segment.

The present *ab initio* study is the third step in our investigation of the static first hyperpolarizability of polymethineimine chains. Although the PPP method can, sometimes, mimic trends in *ab initio* calculations, there are often substantial quantitative discrepancies as we find here. As in the PPP treatment, we examine the chain length dependence of the various tensor components within the CHF scheme. A careful extrapolation procedure, using stability criteria, is carried out to yield reliable asymptotic limits. The nonmonotonic dependence of $\Delta\beta_{zzz}(N)$ upon *N* is quantitatively related to the electronic delocalization along the chain and the asymmetry of the system using new fitting functions. For this component we make a comparison between the UCHF and CHF approaches. An interpretation of our results follows a brief description of the methodology and precedes a concluding section on future directions.

2. Methodology

Calculations of the β tensor were carried out on increasingly large PMI chains built from the repetition in one-direction of the same structural unit (Figure 1). A set of Hartree–Fock 6-31G[29] geometrical parameters defining the unit cell was

TABLE 1: Geometrical Parameters of the PMI Unit Cells Used To Build the Oligomers[a]

	A	B	C	D	E
$R_{C=N}$	1.280	1.264	1.255	1.235	1.220
R_{N-C}	1.380	1.390	1.405	1.425	1.440
R_{C-H}	1.088	1.088	1.088	1.088	1.088
$\alpha_{C=N-C} = \alpha_{N-C=N}$	120.2	120.2	120.2	120.2	120.2
α_{N-C-H}	118.7	118.3	118.0	117.5	117.2
a	2.306	2.302	2.307	2.308	2.309
Δr	0.100	0.126	0.150	0.190	0.220

[a] Bond lengths are given in Å, bond angles in degrees, $\Delta r = R_{N-C} - R_{C=N}$ is the bond length alternation and the other parameters are defined in Figure 1.

obtained by optimization of *all-trans*-PMI chains of increasing size using the Gaussian 92[30] program. In order to maintain the one-dimensional extension of the chains, we have used a model in which the CNC and NCN bond angles are equal. Without some constraints, complete geometry optimization of the all-trans conformers would lead to bent structures because of the stronger electrostatic repulsion between the nitrogen lone pairs than between the CH bonds. It is important to note that the bending can, in principle, be modified and even inverted when the hydrogen atoms are replaced by methyl, phenyl, ... groups. As in the work of Albert *et al.*,[23] where linearity has been assumed, these conformational effects are left for further investigation.

It turns out that the chain length dependence of the PMI geometrical parameters is larger[31] than for polyacetylene[32] and is due to the polarity of the unit cell. We have chosen the parameters of the central unit cell of the octamer as the building block for constructing what we call structure B. The resulting unit cell parameters closely mimic the infinite chain geometry. In this case, the bond length alternation value Δr, given by the bond length difference between the N–C single bond and the C=N double bond, equals 0.126 Å.

In order to address the effects of bond length alternation on the chain length dependence of β we have artificially built several other homologous series of PMI chains based on modified C=N and N–C bond lengths, with the other parameters, including the unit cell length, being held nearly constant. The resulting geometries are displayed in Table 1 with the different structures characterized by the letter A, B, C, D, and E corresponding to $\Delta r = 0.100, 0.126, 0.150, 0.190,$ and 0.220 Å, respectively. In this way we simulate $(AB)_N$ chains presenting different bond length alternation which could, in principle, be obtained upon various chemical substitutions. No simulation of the change in heteroatomicity due to possible substitutions along the backbone were attempted.

The response of a molecule to an homogeneous static electric field $\vec{F}$ can be represented by either of the following two expansions:

$$E(\vec{F}) = E_0 - \vec{\mu}_0 \cdot \vec{F} - \frac{1}{2!}\vec{\vec{\alpha}}:\vec{F}\vec{F} -$$
$$\frac{1}{3!}\vec{\vec{\vec{\beta}}}:\vec{F}\vec{F}\vec{F} - \frac{1}{4!}\vec{\vec{\vec{\vec{\gamma}}}}:\vec{F}\vec{F}\vec{F}\vec{F} - ... \quad (1)$$

$$\vec{\mu}(\vec{F}) = \vec{\mu}_0 + \vec{\vec{\alpha}}\cdot\vec{F} + \frac{1}{2!}\vec{\vec{\vec{\beta}}}:\vec{F}\vec{F} + \frac{1}{3!}\vec{\vec{\vec{\vec{\gamma}}}}:\vec{F}\vec{F}\vec{F} + ... \quad (2)$$

where E_0 is the energy of the molecule in the absence of the electric field, $\vec{\mu}_0$ is the permanent dipole moment, $\vec{\vec{\alpha}}$ is the electric dipole polarizability, and $\vec{\vec{\vec{\beta}}}$ and $\vec{\vec{\vec{\vec{\gamma}}}}$ are the first and second electric dipole hyperpolarizabilities, respectively. Both series have equal coefficients within variational approximation schemes such as the Hartree–Fock (HF) approach and, therefore, the first hyperpolarizability tensor is

$$\vec{\beta} = -\left(\frac{\partial^3 E(\vec{F})}{\partial \vec{F}^3}\right)_{\vec{F}=0} = \left(\frac{\partial^2 \vec{\mu}(\vec{F})}{\partial \vec{F}^2}\right)_{\vec{F}=0} \qquad (3)$$

Calculation of the dipole moment matrix and of the first derivative of the LCAO matrix with respect to an external electric field gives enough information to evaluate the CHF first hyperpolarizability tensor. The first derivatives of the LCAO matrix elements are obtained analytically by the coupled-perturbed Hartree−Fock (CPHF) procedure[33] which has been implemented in the HONDO 95.3 program.[34] This procedure includes field-induced electron reorganizational effects self-consistently in terms of the average Coulomb and Pauli potentials. It is equivalent to the HF finite field technique and to the time-dependent Hartree−Fock (TDHF) approach or the random phase approximation (RPA) in the limit of zero frequency.

From time-independent perturbation theory, the static first hyperpolarizability tensor is given by[35]

$$\vec{\beta} = 6 \sum_j \sum_k \frac{\langle \Psi_0 | \vec{\mu} | \Psi_j \rangle \overline{\langle \Psi_j | \vec{\mu} | \Psi_k \rangle} \langle \Psi_k | \vec{\mu} | \Psi_0 \rangle}{(E_0 - E_j)(E_0 - E_k)} \qquad (4)$$

where Ψ_0 is the ground state wave function of energy E_0, Ψ_j is the jth excited state wave function of energy E_j, $\vec{\mu}$ is the dipole moment operator and

$$\overline{\langle \Psi_j | \vec{\mu} | \Psi_k \rangle} = \langle \Psi_j | \vec{\mu} | \Psi_k \rangle - \langle \Psi_0 | \vec{\mu} | \Psi_0 \rangle \delta_{jk}$$

The UCHF treatment is obtained by using Slater determinants formed from Hartree−Fock orbitals as approximate wave functions while the associated energy is taken to be the sum of the energies of the orbitals in that determinant.[36] In this treatment, the field-induced effects on the electron−electron interactions are not taken into account.[37] Since the excitation energies are given by the orbital energy difference between the unoccupied and occupied one-electron levels, there is no interaction between the excited electron going into the unoccupied orbital and the hole left behind. This leads to an overestimate of the excitation energies and often to an underestimate of the magnitude of $\vec{\beta}$. Within the UCHF scheme, the SOS expression (4) may be transformed into a summation over occupied (i, j) and unoccupied (a, b) levels which, for a closed-shell system, takes the form

$$\vec{\beta} = 12 \sum_{i,j}^{occ} \sum_a^{unocc} \frac{\langle \phi_i | \vec{r} | \phi_a \rangle \langle \phi_j | \vec{r} | \phi_i \rangle \langle \phi_a | \vec{r} | \phi_j \rangle}{(\epsilon_i - \epsilon_a)(\epsilon_j - \epsilon_a)} -$$
$$12 \sum_i^{occ} \sum_{a,b}^{unocc} \frac{\langle \phi_i | \vec{r} | \phi_a \rangle \langle \phi_a | \vec{r} | \phi_b \rangle \langle \phi_b | \vec{r} | \phi_i \rangle}{(\epsilon_i - \epsilon_a)(\epsilon_i - \epsilon_b)} \qquad (5)$$

where ϵ_x is the one-electron energy corresponding to the orbital ϕ_x. The HONDO 95.3[34] program computes the UCHF β by following the algorithm of Fripiat *et al.*[38] that involves a straightforward use of the molecular orbitals and energies calculated by the HF self-consistent field procedure.

In all our calculations we used a split-valence 6-31G atomic basis set.[29] This basis was found to be adequate in the evaluation of α and γ in medium and long polyacetylene (PA) chains.[39] For small donor/acceptor molecules such as p-NA[2] and nitrobenzene,[40] double-zeta quality basis sets have been shown to yield first hyperpolarizabilities that are within about 20% of those obtained when polarization and diffuse functions are added to the basis set. Since this discrepancy is expected to diminish with increasing chain length[39] we judge the 6-31G

basis to be adequate for our calculations except, perhaps, for the smallest PMI chains.

3. Results and Interpretation

3.A. Evolution with Chain Length of the First Hyperpolarizability per Unit Cell and Extrapolation to the Infinite Chain Limit. For all PMI structures we have calculated $\vec{\beta}$ for chains ranging from the monomer to the eicosamer (20 CH=N units). The nonzero tensor components obtained at the CHF/6-31G level of approximation are listed in Tables 2 and 3 for structures B and E. Table 4 lists β_{zzz} for the A, C, and D structures. For sufficiently long chains of structures B and E, the longitudinal component, β_{zzz}, is the largest. At $N = 20$ the β_{xzz} component is smaller in magnitude by roughly a factor of 2 while the other components are essentially negligible. The difference is even more pronounced (see below) when one considers $\Delta\beta_{zzz}$ and $\Delta\beta_{xzz}$. This predominance of the longitudinal component is due to electron delocalization along the chain. With the exception of β_{zzz}, and β_{xxz} (for the E structure), the β tensor components increase monotonically with chain length. β_{zzz} is negative initially, goes through a maximum as N increases, and decreases continuously after that to a negative value at long chain lengths. The maximum shifts steadily from about $N = 7$ in the A structure of PMI to between $N = 1$ and $N = 2$ in the oligomers of structure E. For comparison, the longitudinal component of the dipole moment is negative, whatever the size and structure of the chain, and it grows monotonically.

We are interested in the first hyperpolarizability per unit cell as a function of chain length. Two different definitions are commonly used for this quantity, both of which must lead to the same asymptotic limit. For the most rapid convergence with N we choose $\Delta\beta(N) = \beta(N) - \beta(N - 1)$ rather than $\beta(N)/N$. Figures 2 and 3 show the evolution of $\Delta\vec{\beta}$ with chain length for the structures B and E (all nonzero tensor components); Figure 4 shows the β_{zzz} component for all five series. Two different behaviors are observed: one for $\Delta\beta_{zzz}$ and one for all the other components. The latter approach their asymptotic limit monotonically. On the other hand, $\Delta\beta_{zzz}$ initially increases toward a maximum and then decreases, becomes negative and, finally, tends toward the polymeric value. The leveling off to the asymptotic limit is slowest for β_{xzz} and β_{zzz} because the electrons are delocalized primarily in the longitudinal (z) direction. From Figure 4 we see that as the conjugation increases (*i.e.* the bond alternation decreases) the maximum in $\Delta\beta_{zzz}$ increases in height and shifts to larger N. At the same time the approach to saturation is slower and the magnitude of the limiting infinite chain value is larger. The saturation behaviour of the individual structures is similar to that found for the linear polarizability and second hyperpolarizability of other conjugated polymers.[32,39,41−44]

In order to obtain the $\Delta\beta_{zzz}$ asymptotic limit, it is clear from Figures 2−4 that an extrapolation is necessary. Three different functional forms have been employed here for that purpose:

$$\Delta\beta_{zzz}(N) = a + \frac{b}{N} + \frac{c}{N^2} \qquad (6a)$$

$$\Delta\beta_{zzz}(N) = a - be^{-cN} \qquad (6b)$$

$$\Delta\beta_{zzz}(N) = \frac{a}{1 + be^{-cN}} \qquad (6c)$$

The 1/N power series (eq 6a) was originally proposed[45] to fit total and orbital energies of polyacetylene. It has been applied

all-trans-Polymethineimine Oligomers

J. Phys. Chem. A, Vol. 101, No. 17, 1997 **3161**

TABLE 2: CHF/6-31G β Tensor Components of PMI Chains of Structure B as a Function of the Number of Unit Cells (N)

N	β_{xxx}	β_{xxz}	β_{xzz}	β_{xyy}	β_{yyz}	β_{zzz}
1	51.220	15.541	15.678	7.124	8.610	−10.25
2	94.947	9.445	59.774	10.733	20.999	15.45
3	131.331	9.808	144.964	15.314	37.878	81.67
4	167.511	14.406	279.036	20.133	57.704	182.23
5	203.859	24.398	461.720	25.127	79.648	276.10
6	240.633	39.871	687.546	30.239	103.101	308.18
7	277.901	60.346	948.724	35.432	127.618	229.59
8	315.633	85.091	1237.343	40.679	152.884	8.42
9	353.770	113.332	1546.587	45.961	178.679	−368.42
10	392.246	144.376	1871.101	51.268	204.853	−899.34
11	430.991	177.626	2206.763	56.590	231.302	−1573.55
12	469.959	212.620	2550.697	61.925	257.954	−2375.80
13	509.098	248.977	2900.688	67.268	284.759	−3289.25
14	548.374	286.406	3255.224	72.617	311.681	−4297.71
15	587.761	324.690	3613.196	77.970	338.690	−5386.20
16	627.234	363.649	3973.799	83.326	365.768	−6541.83
17	666.777	403.149	4336.438	88.686	392.901	−7753.50
18	706.377	443.089	4700.678	94.045	420.078	−9011.90
19	746.026	483.393	5066.258	99.408	447.289	−10309.23
20	785.709	523.980	5432.801	104.772	474.531	−11639.09
$\Delta\beta(\infty)$	39.84 ± 0.02	41.76 ± 0.36	370.24 ± 1.17	5.37 ± 0.00	27.36 ± 0.04	−1461 ± 51

[a] In the last row we give the corresponding value per unit cell extrapolated to the infinite chain limit following the procedure described in the text. All the values are in au (1.0 au = 3.206×10^{-53} C^3 m^3 J^{-2} = 8.641×10^{-33} esu).

TABLE 3: CHF/6-31G β Tensor Components of PMI Chains of Structure E as a Function of the Number of Unit Cells (N)

N	β_{xxx}	β_{xxz}	β_{xzz}	β_{xyy}	β_{yyz}	β_{zzz}
1	53.176	16.040	13.783	6.566	7.698	−11.54
2	97.990	8.710	48.900	9.774	18.338	−11.66
3	134.680	5.126	105.307	13.706	32.229	−29.72
4	170.681	2.080	180.394	17.766	47.932	−75.74
5	206.261	−0.102	269.852	21.921	64.828	−157.56
6	241.651	−1.447	369.631	26.141	82.516	−275.10
7	276.950	−2.083	476.586	30.404	100.732	−428.83
8	312.208	−2.158	588.490	34.698	119.306	−610.54
9	347.445	−1.803	703.817	39.012	138.125	−815.97
10	382.672	−1.121	821.543	43.340	157.116	−1040.35
11	417.894	−0.193	940.977	47.678	176.230	−1279.64
12	453.112	0.924	1061.649	52.025	195.435	−1530.59
13	488.330	2.185	1183.243	56.376	214.706	−1790.68
14	523.545	3.556	1305.515	60.732	234.027	−2057.91
15	558.759	5.011	1428.312	65.090	253.387	−2330.77
16	593.972	6.537	1551.523	69.452	272.777	−2608.10
17	629.184	8.114	1675.049	73.815	292.192	−2889.01
18	664.394	9.734	1798.832	78.180	311.625	−3172.79
19	699.603	11.390	1922.823	82.547	331.076	−3458.90
20	734.811	13.074	2046.984	86.914	350.539	−3746.92
$\Delta\beta(\infty)$	35.11 ± 0.10	1.79 ± 0.06	124.82 ± 0.19	4.37 ± 0.00	19.52 ± 0.02	−293.4 ± 2.0

[a] In the last row we give the corresponding value per unit cell extrapolated to the infinite chain limit following the procedure described in the text. All the values are given in au (see Table 2 footnote for conversion to other units).

many times since then to fit the (hyper)polarizability per unit cell (or its logarithm) of oligomeric chains.[32,39,41,43] This expression is supported by the fact that the total Hartree−Fock energy per unit cell can formally be written as a power series in $1/N$.[46] In recent work,[44] it has been shown that the exponential function in eq 6b leads to extrapolated linear polarizabilities per unit cell that are in good agreement with values obtained directly from crystal orbital calculations. Finally, the right-hand side of the third fitting function (eq 6c) is the solution of the *logistic equation*[47] which has been used historically to describe the growth of a population that is limited by food supply or other circumstances. Obviously, other forms such as Padé approximants[46] could be considered.

The set of N values used in the least-squares fit of eqs 6a−c is arbitrary as long as there are at least as many points as there are parameters. It has recently been noted[32] that this freedom can be utilized to monitor the stability and, hence, the reliability of the extrapolated result. In particular, one can define a consecutive set of points by the maximum N (N_{max}) and the minimum N (N_{min}) so that $N_{max} - N_{min} = k + p$, where $k + 1$ is the number of fitting parameters and p is the number of degrees of freedom. For fixed k and N_{max}, an additional degree of freedom is added each time N_{min} is reduced by unity. In this way one can determine the stability with respect to the size of the shortest chain in the data set. In the case of eq 6a one can also examine the stability with respect to varying the order of the polynomial. The use of different fitting functions here enables us to assess the accuracy of the asymptotic value.

Table 5 lists the extrapolated longitudinal first hyperpolarizability per unit cell obtained with different N_{max} and p in eqs 6a−c. In order to get a good least-squares fit, experience dictates that one should require $p \geq k$, as we have done here. Evidently, the polynomial fit (6a) is not very stable compared to the other two functions with respect to varying p and N_{max}. We tried a cubic series in $1/N$ as well with similar results. This simply means that for this particular property, and this particular system, longer chains are needed to achieve good precision.

TABLE 4: CHF/6-31G β_{zzz} of PMI Chains of Structure A, C, and D as a Function of the Number of Unit Cells (N)

N	A	C	D
1	−9.58	−10.30	−10.91
2	27.05	7.42	−4.18
3	139.49	44.22	−3.94
4	341.20	86.79	−23.79
5	590.47	101.79	−81.29
6	805.95	54.62	−187.30
7	896.43	−79.06	−344.95
8	786.11	−310.20	−551.55
9	426.55	−638.57	−801.38
10	−202.93	−1056.89	−1087.68
11	−1101.72	−1554.35	−1403.86
12	−2255.28	−2119.65	−1744.24
13	−3641.08	−2741.70	−2103.95
14	−5233.5	−3410.71	−2479.11
15	−7006.69	−4118.34	−2866.59
16	−8936.21	−4857.63	−3263.93
17	−10999.87	−5622.87	−3669.19
18	−13178.14	−6409.52	−4080.88
19	−15453.99	−7213.71	−4497.78
20	−17812.82	−8032.08	−4918.96
$\Delta\beta_{zzz}(\infty)$	−2753 ± 129	−869 ± 28	−434 ± 7

[a] In the last row we give the corresponding value per unit cell extrapolated to the infinite chain limit following the procedure described in the text. All the values are given in au (see Table 2 caption for conversion to other units).
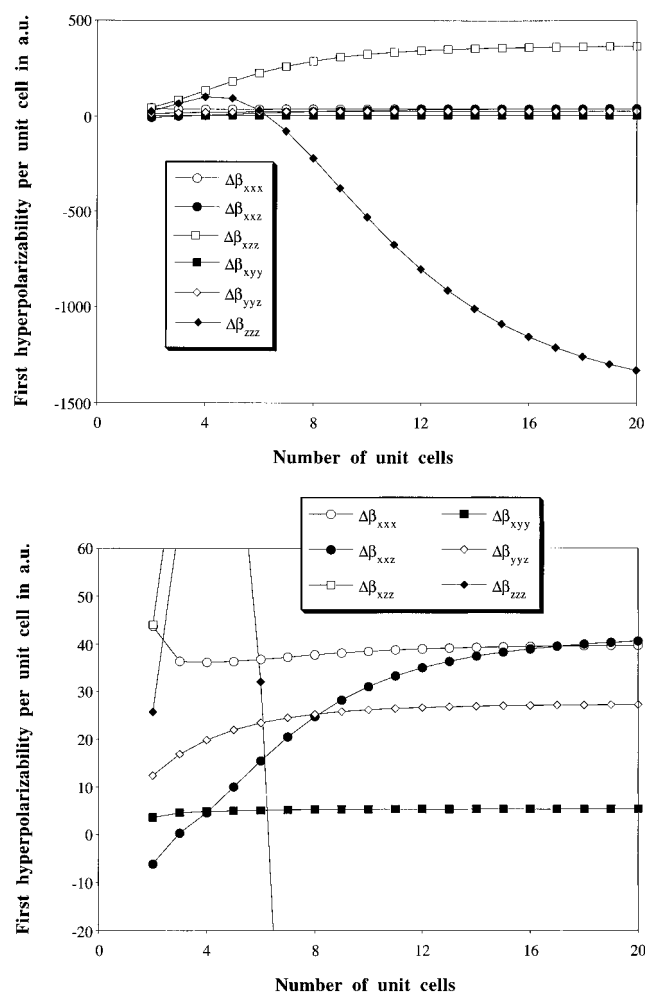

Figure 2. Evolution with chain length of the CHF/6-31G first hyperpolarizability per unit cell, $\Delta\vec{\vec{\beta}}$, of PMI chains of structure B. The lower panel is a blow-up of the −20 to 60 au region.

However, the two other forms, and particularly eq 6b, are much better behaved. Setting $N_{max} = 20$, the extrapolated values for B structure obtained from eq 6b range between −1493 and −1512 au for $p = 2−7$ with no jump between successive values
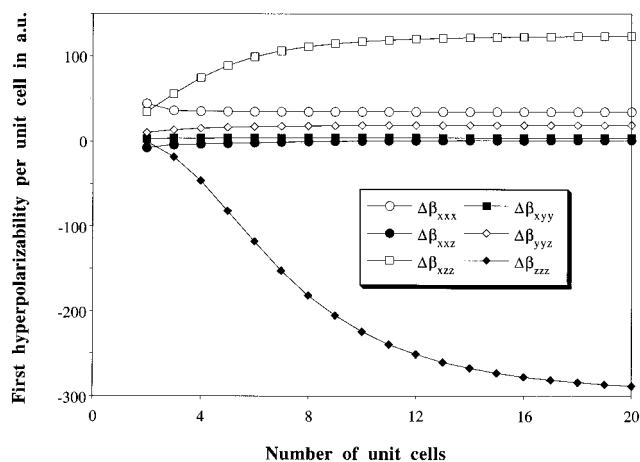

Figure 3. Evolution with chain length of the CHF/6-31G first hyperpolarizability per unit cell, $\Delta\vec{\vec{\beta}}$, of PMI chains of structure E.
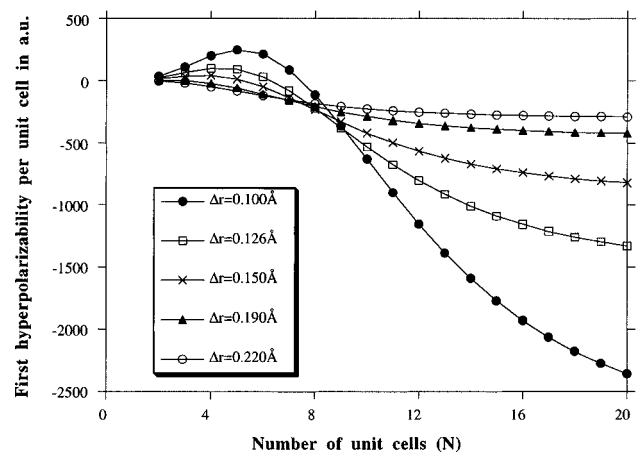

Figure 4. Bond length alternation effect on the chain length dependence of the CHF/6-31G $\Delta\beta_{zzz}$ of PMI chains.

greater than $\epsilon = \pm15$ au. Applying the same stability criterion to the extrapolations using eq 6c, the range is −1455 to −1410 au, for $p = 2−6$. Thus, the fits for both functional forms are consistent with $\Delta\beta_{zzz}(\infty) = −1461 \pm 51$ au which we take as the asymptotic value. Note that this result is consistent (in the region of stability) with the three sets of extrapolations for which p is fixed and N_{max} is variable. It appears to be consistent as well with trends in the polynomial fits. For structure E the dependence upon N_{max} and p is much weaker. Using a stability criterion of $\epsilon = \pm2.0$ au, we find $\Delta\beta_{zzz}(\infty) = −293.4 \pm 2.0$ au.

Although the largest chain lengths already provide accurate estimates of the polymeric values for the other $\Delta\beta$ tensor components of the chains of structures B and E, similar procedures have been adopted. For structure B the magnitude of the ratio $\Delta\beta_{zzz}(\infty)/\Delta\beta_{xzz}(\infty)$ is 3.95 whereas for structure E it is 2.35. The polymeric values of $\Delta\beta_x$ ($\beta_x = \beta_{xxx} + \beta_{xyy} + \beta_{xzz}$) and $\Delta\beta_z$ ($\beta_z = \beta_{zxx} + \beta_{zyy} + \beta_{zzz}$) are 415.45 ± 1.19 and −1392 ± 52 au, respectively, in the case of B structure PMI while $\Delta\beta_x = 164.30 \pm 0.29$ au and $\Delta\beta_z = −272.1 \pm 2.1$ au in the case of the E structure. The same approach has been followed for estimating the $\Delta\beta_{zzz}(\infty)$ values in the A-, C-, and D-structure PMI (Table 4).

3.B. Role of Bond and Atomic Alternation in Determining $\Delta\beta_{zzz}(N)$ vs N. Connection with Electronic Asymmetry and Delocalization. By considering the behavior of $\beta_{zzz}(N)$ as a function of the degree of bond alternation and atomic alternation (heteroatomicity) one can gain insight into the role of asymmetry and electron delocalization in determining the chain length dependence. From Figure 4 it is evident that the plot of $\Delta\beta_{zzz}(N)$ vs N becomes increasingly flat as the degree of bond alternation increases. The smallest bond alternation produces

all-trans-Polymethineimine Oligomers

J. Phys. Chem. A, Vol. 101, No. 17, 1997 **3163**

TABLE 5: Extrapolated CHF/6-31G $\Delta\beta_{zzz}$ Values Obtained Using Three Different Analytical Forms for the Fitting Function and a Variety of Data Sets

no. of points	data range	$a + (b/N) + (c/N^2)$	$a - be^{-cN}$	$a/(1 + be^{-cN})$
		Structure B		
12	9–20	−2146	−1554	−1353
11	10–20	−2011	−1528	−1394
10	11–20	−1892	−1512	−1393
9	12–20	−1792	−1503	−1410
8	13–20	−1709	−1497	−1424
7	14–20	−1644	−1495	−1436
6	15–20	−1590	−1493	−1446
5	16–20	−1549	−1493	−1455
7	14–20	−1644	−1495	−1436
7	13–19	−1750	−1499	−1413
7	12–18	−1893	−1510	−1383
7	11–17	−2074	−1535	−1342
7	10–16	−2294	−1589	−1286
6	15–20	−1590	−1493	−1446
6	14–19	−1680	−1495	−1427
6	13–18	−1798	−1501	−1401
6	12–17	−1956	−1517	−1366
6	11–16	−2153	−1550	−1318
5	16–20	−1549	−1493	−1455
5	15–19	−1619	−1493	−1438
5	14–18	−1726	−1498	−1417
5	13–17	−1853	−1505	−1386
5	12–16	−2026	−1525	−1345
		Structure E		
12	9–20	−306.5	−294.5	−291.3
11	10–20	−303.9	−295.4	−292.9
10	11–20	−296.5	−295.2	−293.4
9	12–20	−291.2	−295.2	−293.8
8	13–20	−284.2	−294.9	−293.9
7	14–20	−271.6	−293.9	−293.2
6	15–20	−247.6	−292.2	−291.8
6	15–20	−247.6	−292.2	−291.8
6	14–19	−276.9	−294.6	−293.7
6	13–18	−318.4	−301.0	−298.7
6	12–17	−316.2	−298.7	−295.8
6	11–16	−303.0	−293.5	−290.2

[a] All values are given in au.

the highest maximum and the largest (in magnitude) asymptotic value. We associate a decrease of bond alternation with an increase in the electron delocalization. In addition, however, the decrease in bond alternation is also associated with a decrease in the asymmetry of the backbone. This can be seen from ordinary Hückel[24] calculations where the *asymptotic* $\Delta\beta_{zzz}(\infty)$ approaches zero as the two bond parameters approach one another for fixed atomic alternancy. Presumably, such behavior is not seen here because the bond alternancy is too large even for structure A. Hückel calculations behave similarly to the *ab initio* ones for large bond alternancy in which one, despite the large asymmetry, $\Delta\beta_{zzz}(\infty)$ is small due to strong electron localization.

The heteroatomicity, likewise, affects both the backbone (or unit cell) asymmetry and the electron delocalization. Ordinary Hückel calculations[24] and recent CHF/6-31G investigations[48] demonstrate that increasing the heteroatomicity (for fixed bond length alternation) decreases the longitudinal linear polarizability, which we interpret as being due to a decrease in electron delocalization. On the other hand, the asymptotic longitudinal first hyperpolarizability may either increase or decrease in magnitude. If it decreases, then the electron localization is dominant; if it increases, the asymmetry is dominant.

Besides the backbone asymmetry there is also a chain end asymmetry. These two different types of asymmetry are indicated most clearly by the data in Tables 2–4 which show a reversal in the sign of β_{zzz} for oligomers of structures A–C in the region $N = 7$–10. The backbone asymmetry is dominant

for larger N while the chain end asymmetry is dominant for smaller N. Of course, the chain end asymmetry would not exist if there were no heteroatomicity; but when it does exist the bond alternation will influence its magnitude as ordinary Hückel calculations[24] reveal.

As illustrated in Figure 4, the effect of increasing electron delocalization is to magnify the hump in the dromedary back curve of $\Delta\beta_{zzz}(N)$ vs N and to push the sign reversal to larger N. Thus, the detailed shape of this curve arises from combined effects of asymmetry and electron delocalization. This situation is represented mathematically in the next section by writing the hyperpolarizability per unit cell as a simple product of two functions one representing the electron delocalization and the other the asymmetry.

3.C. Quantitative Fit of the Longitudinal Hyperpolarizability per Unit Cell vs Chain Length. It is of interest to obtain a quantitative fit for the dependence of the longitudinal hyperpolarizability per unit cell on chain length. To this end we test the following two forms each of which is a simple product of a delocalization function multiplied by an asymmetry function:

$$\frac{\beta_{zzz}(N)}{N} = \left[\frac{m_1}{1 + m_2 e^{-m_3 N}}\right]\left(1 + \frac{m_5}{N}\right) \qquad (7a)$$

$$\frac{\beta_{zzz}(N)}{N} = \left[m_1 + m_2 \tanh\left(\frac{N - m_3}{m_4}\right)\right]\left(1 + \frac{m_5}{N}\right) \qquad (7b)$$

We have chosen to fit $\beta_{zzz}(N)/N$ here, rather than $\Delta\beta_{zzz}(N)$, in order to emphasize chain end asymmetry. The contribution of chain ends is largely cancelled (see also below) in forming $\Delta\beta_{zzz}(N)$. In eqs 7a and 7b the quantity $(1 + m_5/N)$ is the asymmetry function. Except for a proportionality factor the constant term represents the backbone asymmetry while the $1/N$ term represents the chain end contribution. This assumes that the effect of delocalization on both types of asymmetry is the same. It is also assumed, for the sake of simplicity, that higher powers in $1/N$ can be omitted. Note that if m_5 is negative, then the asymmetry gives rise to a sign reversal at $N = |m_5|$.

The delocalization function in eq 7a is the solution of the logistic equation, which we have used previously in this paper to describe the asymptotic (and near asymptotic) behavior of $\Delta\beta_{zzz}(N)$. From the fact that this function is slowly varying at large N it is easy to show that the two usages of the logistic equation (eqs 6c and 7a) are consistent with one another. Furthermore, the shape of this function is appropriate for all N since it qualitatively describes the complete chain length dependence[41] of both the linear polarizability and the second hyperpolarizability of centrosymmetric oligomers (including the possibility of a point of inflection). As a measure of the overall delocalization effect we use the difference, DLOC, between the value of the delocalization function at $N = \infty$ and at $N = 1$. Since the value at $N = 1$ turns out to be small compared to the value at $N = \infty$, DLOC is approximatively m_1. The delocalization or conjugation length which yields some specified fraction of DLOC, is determined essentially by m_2 and m_3.

If m_2 is positive, as it is here, then the delocalization function will have the same sign for all N. Thus, eq 7a cannot reproduce the sign reversal that occurs at $N = 1$ for the A–C structures of PMI. For this reason the point $N = 1$ is not included in the data set used for the fitting.

The analysis of the delocalization function in eq 7b is similar to the above. In this case DLOC is approximately $m_1 + m_2$, the electron delocalization effects are described by m_2 as well as m_3 and m_4, and the inflection point is determined by m_3. m_1/m_2 and m_4 are associated with the amplitude and rate of the
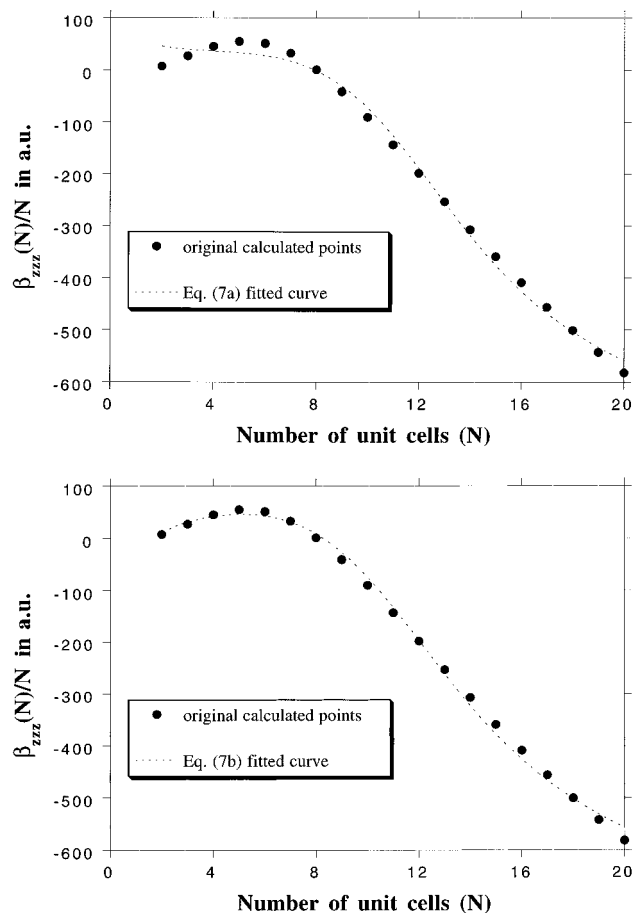
Figure 5. Comparison of calculated CHF/6-31G $\beta_{zzz}(N)/N$ vs N for PMI chains of B structure with the curve obtained by a least-squares fit to eqs 7a and 7b.

TABLE 6: Least-Squares Parameters for the Fit of Eq 7b to the CHF/6-31G $\beta_{zzz}(N)/N$ for PMI Chains of Structures A−E[a]

	A	B	C	D	E
DLOC	−1851	−1041	−645	−347	−228
N_{90}^c	19	20	20	25	21
$m_1 + m_2$	−1830	−1022	−629	−326	−220
m_1/m_2	0.907	0.853	0.772	0.468	0.436
m_3	11.5	10.8	10.0	7.4	6.2
m_4	6.3	7.0	7.8	10.0	10.1
m_5	−9.8	−7.9	−6.3	−3.3	−1.6

[a] The $N = 2$−20 data have been utilized. The quantities DLOC and N_{90}^c are defined in the text. DLOC and $m_1 + m_2$ have units of first hyperpolarizability (au) while all the other quantities are dimensionless.

$\beta_{zzz}(N)/N$ variation with chain length, respectively. Although m_1 and m_2 have the same sign, the delocalization function can accommodate a change in sign at small N because the tanh factor varies in sign.

Figure 5 shows representative least-squares fits for the B structure of PMI using the points $N = 2$−20. Reasonable results are obtained for eq 7b but the fit of eq 7a is poor, particularly in the vicinity of the maximum. Consequently, we do not consider the latter any further. Fitting parameters obtained for the five PMI structures using eq 7b are reported in Table 6. As expected, DLOC is given quite accurately by $m_1 + m_2$. This quantity decreases sharply with increasing bond alternation. In addition, as the bond alternation increases the backbone asymmetry increases markedly with respect to the chain end asymmetry (1 vs $|m_5|$) and the point of inflection (m_3) moves to significantly smaller N. m_4 monotonically increases with the bond length alternation showing that the rate of variation of $\beta_{zzz}(N)/N$ vs N decreases concomitantly. On the other hand,
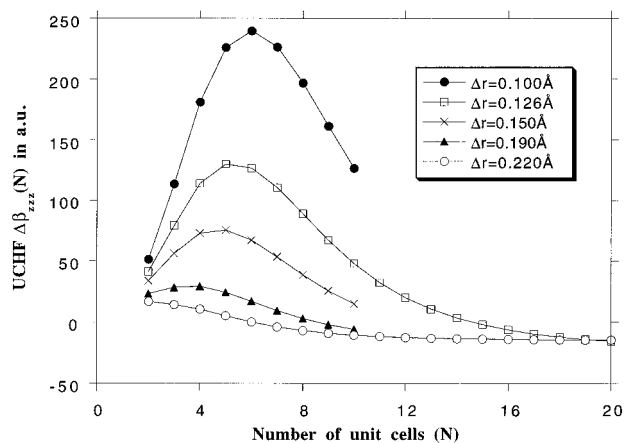

Figure 6. Evolution with chain length of UCHF/6-31G $\Delta\beta_{zzz}$ as a function of the bond length alternation.
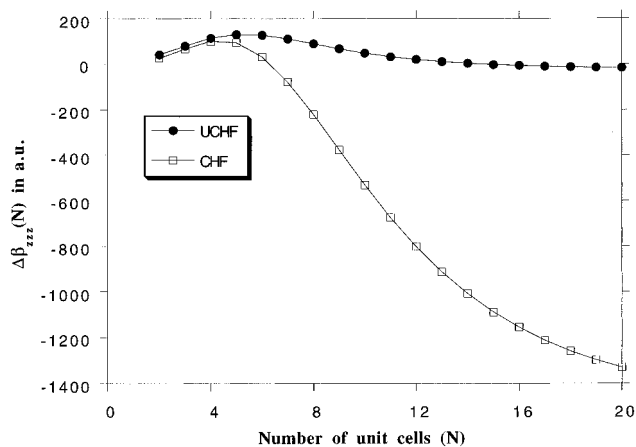

Figure 7. Comparison between the UCHF and CHF values for the evolution of the 6-31G $\Delta\beta_{zzz}(N)$ as a function of the chain length for the B structure ($\Delta r = 0.126$ Å) PMI chains.

the conjugation length (defined to yield 90% of DLOC and, therefore called N_{90}^c) is essentially the same for each of the structures. All of these features are consistent (as far as they are applicable) with the discussion of the previous subsection. They show also that eq 7b can be used quantitatively to describe the electron delocalization and asymmetry effects on the chain length behavior of $\beta_{zzz}(N)$.

3.D. Uncoupled vs Coupled Hartree−Fock Approximations for $\Delta\beta_{zzz}(N)$. We have applied the uncoupled Hartree−Fock approximation to calculate $\Delta\beta_{zzz}(N)$ for the five PMI structures. Figure 6 displays the $\Delta\beta_{zzz}(N)$ evolution with chain length and a typical plot comparing UCHF/6-31G with CHF/6-31G in the case of the B structure is shown as Figure 7. Although UCHF does fairly well for small oligomers the chain length dependence is not correct beyond the position of the maximum; the UCHF curve is, clearly, much too flat. These *ab initio* results confirm the general conclusion of our previous PPP treatment[25] based on the Tavan and Schulten parametrization. The lack of field-induced effects on the electron−electron interactions in the UCHF calculations leads to the same results as an increase of alternation, *i.e.* $\Delta\beta_{zzz}(\infty)$ is smaller and the saturation with chain length is faster. Similar observations have already been made for the linear polarizability.[44] In addition, the sign change in $\Delta\beta_{zzz}(N)$ occurs at much larger N, indicating a description of the asymmetry overly biased toward the chain end contribution.

4. Future Directions

PMI is an example of a polymer that has an asymmetric unit cell and thereby exhibits a static longitudinal first hyperpolar-

all-trans-Polymethineimine Oligomers

J. Phys. Chem. A, Vol. 101, No. 17, 1997 **3165**

izability. Each unit cell contains the donor and the acceptor while, at the same time, being part of the conjugated backbone that generates a unique behavior for $\Delta\beta_{zzz}(N)$ vs N which exhibits a "dromedary back" shape. The magnitude of $\Delta\beta_{zzz}(\infty)$ is -1461 au per [CH=N] unit for the B structure, which is the best representation of the all-trans stereoregular chain. This is comparable to the values in standard push−pull systems. For examples, CHF/6-31G calculations[49] give $\beta_{zzz} = -4280$ au for $NH_2[CH=CH]_3NO_2$ and -13750 au for $NH_2[CH=CH]_5NO_2$, or -1070 and -2292 au, respectively, per pair of backbone atoms. Thus, PMI shows promise as an NLO material, particularly when one considers the possibilities for tuning by chemical substitution.

The calculations presented here constitute just the first step in an *ab initio* investigation of the NLO properties of this interesting polymer. Besides frequency dispersion, we have yet to examine the role of electron correlation,[50] or of the associated choice of an atomic basis set, or of vibrational distortions,[51] or the interactions with the medium.[22] Recent work has shown that each of these phenomena can, individually, cause the hyperpolarizability to change by a factor of 2−3 and, in some cases, an order of magnitude. Of course, the crystal packing is critical; if it is centrosymmetric then the first hyperpolarizability will cancel out. Because of the polar nature of the unit cell there is reason to believe that vibrations and interchain interactions may be especially important as well.

References and Notes

(1) André, J. M.; Delhalle, J. *Chem. Rev.* **1991**, *91*, 843−865.

(2) Kanis, D. R.; Ratner, M. A.; Marks, T. J. *Chem. Rev.* **1994**, *94*, 195−242.

(3) Brédas, J. L.; Adant, C.; Tackx, P.; Persoons, A.; Pierce, B. M. *Chem. Rev.* **1994**, *94*, 243−278.

(4) Meyers, F.; Brédas, J. L. *Int. J. Quantum Chem.* **1992**, *42*, 159−1614.

(5) Meyers, F.; Brédas, J. L.; Zyss, J. *J. Am. Chem. Soc.* **1992**, *114*, 2194−2921.

(6) Tsunekawa, T.; Yamaguchi, K. *Chem. Phys. Letters* **1992**, *190*, 533−538.

(7) Morley, J. O.; Pavlides, P.; Pugh, D. *Int. J. Quantum Chem.* **1992**, *43*, 7−26.

(8) Dehu, C.; Meyers, F.; Brédas, J. L. *J. Am. Chem. Soc.* **1993**, *115*, 6198−6206.

(9) Morley, J. O. *Int. J. Quantum Chem.* **1993**, *46*, 19−26.

(10) Morley, J. O. *J. Phys. Chem.* **1995**, *99*, 10166−10174.

(11) Marder, S. R.; Gorman, C. B.; Tiemann, B. G.; Cheng, L. T. *J. Am. Chem. Soc.* **1993**, *115*, 3006−3007.

(12) Risser, S. M.; Beratan, D. N.; Marder, S. R. *J. Am. Chem. Soc.* **1993**, *115*, 7719−7728.

(13) Ortiz, R.; Marder, S. R.; Cheng, L. T.; Tiemann, B. G.; Cavagnero, S.; Ziller, J. W. *J. Chem. Soc., Chem. Commun.* **1994**, 2263−2264.

(14) Oudar, J. L.; Chemla, D. S. *J. Chem. Phys.* **1977**, *66*, 2664−2668.

(15) Oudar, J. L. *J. Chem. Phys.* **1977**, *67*, 446−447.

(16) Meyers, F.; Marder, S. R.; Pierce, B. M.; Brédas, J. L. *Chem. Phys. Lett.* **1994**, *228*, 171−176.

(17) Meyers, F.; Marder, S. R.; Pierce, B. M.; Brédas, J. L. *J. Am. Chem. Soc.* **1994**, *116*, 10703−10714.

(18) Marder, S. R.; Gorman, C. B.; Meyers, F.; Perry, J. W.; Bourhill, G.; Brédas, J. L.; Pierce, B. M. *Science* **1994**, *265*, 632−635.

(19) Gorman, C. B.; Marder, S. R. *Chem. Mater.* **1995**, *7*, 215−220.

(20) Dehu, C.; Meyers, F.; Hendrickx, E.; Clays, K.; Persoons, A.; Marder, S. R.; Brédas, J. L. *J. Am. Chem. Soc.* **1995**, *117*, 10127−10128.

(21) Kirtman, B. *Int. J. Quantum Chem.* **1992**, *43*, 147−158.

(22) Kirtman B. In *Theoretical and Computational Modeling of NLO and Electronic Materials*; Karna, S. P., Yeates, A. T., Eds.; ACS Symposium Series 628; American Chemical Society: Washington, DC, 1996; p 58 and references therein.

(23) Albert, I. D. L.; Das, P. K.; Ramasesha, S. *Chem. Phys. Lett.* **1991**, *176*, 217−224.

(24) Champagne, B.; Jacquemin, D.; André, J. M. *SPIE Proc.* **1995**, *2527*, 71−81.

(25) Jacquemin, D.; Champagne, B.; André, J. M.; Kirtman, B. *Chem. Phys.* **1966**, *213*, 217−228.

(26) Sales, T. R. M.; de Melo, C. P.; Dos Santos, M. C. *Synth. Met.* **1991**, *41−43*, 3751−3754.

(27) Wöhrle, D. *Tetrahedron Lett.* **1971**, 22, 1969−1970.

(28) Wöhrle, D. *Makromol. Chem.* **1974**, *275*, 1751.

(29) Ditchfield, R.; Hehre, W. J.; Pople, J. A. *J. Chem. Phys.* **1971**, *54*, 724−728.

(30) *Gaussian 92*; Frish, M. J.; Trucks, G. W., Head-Gordon, M.; Gill, P. W. M.; Wong, M. W.; Foresman, J. B.; Jonhson, B. G.; Schlegel, H. B.; Robb, M. A.; Replogle, E.S.; Gomperts, R.; Andrès, J. L.; Raghavachari, K.; Binkley, J. S.; Gonzales, C.; Martin, R. L.; Fox, D. J.; DeFrees, D. J., Baker, J.; Stewart, J. J. P.; Pople, J. A. Gaussian Inc., Carnergie-Mellon University, Pittsburgh, 1992.

(31) Jacquemin, D., unpublished results.

(32) Kirtman, B.; Toto, J. L.; Robins, K. A.; Hasan, M. *J. Chem. Phys.* **1995**, *102*, 5350−5355.

(33) Dykstra, C. E.; Jasien, P. G. *Chem. Phys. Lett.* **1984**, *109*, 388−393. Karna, S. P.; Dupuis, M. *J. Comput. Chem.* **1991**, *12*, 487−504.

(34) Dupuis, M.; Marquez, A.; Davidson, E. R. *HONDO 95.3 from CHEM-Station*; IBM Corp., Neighborhood Road, Kingston, NY 12401; 1995.

(35) Orr, B. J.; Ward, J. F. *Mol. Phys.* **1971**, *20*, 513−526. Bishop, D. M. *J. Chem. Phys.* **1994**, *100*, 6535−6542.

(36) André, J. M.; Barbier, C.; Bodart, V. P.; Delhalle, J. In *Nonlinear Optical Properties of Organic Molecules and Crystals*; Chemla, D. S., Zyss, J., Eds.; Academic: New York, 1987; Vol. 2, pp 137−158.

(37) Dalgarno, A.; McNamee, J. M. *J. Chem. Phys.* **1961**, *35*, 1517−1518. Langhoff, P. W.; Karplus, M.; Hurst, R. P. *J. Chem. Phys.* **1966**, *44*, 505−514. Caves, T. C.; Karplus, M. *J. Chem. Phys.* **1969**, *50*, 3649−3661.

(38) Fripiat, J. G.; Barbier, C.; Bodart, V. P.; André, J. M. *J. Comput. Chem.* **1986**, *7*, 756−760. As a caution for HONDO 95.3 users, the sign convention for μ and β(UCHF) is inconsistent. The β(UCHF) values have then been multiplied by -1.

(39) Hurst, G. J. B.; Dupuis, M.; Clementi, E. *J. Chem. Phys.* **1988**, *89*, 385−395.

(40) Daniel, C.; Dupuis, M. *Chem. Phys. Lett.* **1990**, *171*, 209−216.

(41) Kirtman, B. *Int. J. Quantum Chem.* **1989**, *36*, 119−125. Kirtman, B.; Hasan, M. *Chem. Phys. Lett.* **1989**, *157*, 123−128.

(42) Kirtman, B. *Int. J. Quantum Chem.* **1992**, *42*, 147−158.

(43) Kirtman, B.; Hasan, M. *J. Chem. Phys.* **1992**, *96*, 470−479.

(44) Champagne, B.; Mosley, D. H.; André, J. M. *Int. J. Quantum Chem.* **1993**, *S27*, 667−686. Champagne, B.; Mosley, D. H.; André, J. M. *J. Chem. Phys.* **1994**, *100*, 2034−2043.

(45) Kirtman, B.; Nilsson, W. B.; Palke, W. E. *Solid State Commun.* **1983**, *46*, 791−795.

(46) Cioslowski, J.; Lepetit, M. B. *J. Chem. Phys.* **1991**, *95*, 3536−3547.

(47) Edwards, C. H. Jr.; Penney, D. E. *Differential Equations and Boundary Value Problems−Computing and Modeling*; Prentice Hall: Englewood Cliffs, NJ, 1996; Chapter 2, pp 70−76.

(48) Jacquemin, D.; Champagne, B.; André, J. M., *Synth. Met.*, **1996**, *80*, 205−210.

(49) To be published.

(50) Toto, T. T.; Toto, J. L.; de Melo, C. P.; Hasan, M.; Kirtman, B. *Chem. Phys. Lett.* **1995**, *244*, 59−64. Toto, J. L.; Toto, T. T.; de Melo, C. P. *Chem. Phys. Lett.* **1995**, *245*, 660−664. Toto, J. L.; Toto, T. T.; de Melo, C. P.; Robins, K. A. *J. Chem. Phys.* **1995**, *102*, 8048−8052. Champagne, B.; Mosley, D. H. *J. Chem. Phys.* **1996**, *105*, 3592−3602. Jacquemin, D.; Champagne, B.; André, J. M., *J. Molec. Struct. (THEOCHEM)*, in press.

(51) Champagne, B.; Perpète, E. A.; André, J. M. *J. Chem. Phys.* **1994**, *101*, 10796−10807. Champagne, B.; Perpète, E. A.; André, J. M.; Kirtman, B. *J. Chem. Soc., Faraday Trans.* **1995**, *91*, 1641−1646. Kirtman, B.; Champagne, B.; André, J. M. *J. Chem. Phys.* **1996**, *104*, 4125−4136. Champagne, B.; Perpète, E. A.; André, J. M.; Kirtman, B. *Synth. Met.*, in press.